同種骨移植のための Bone Bank Network

名古屋大学整形外科

坂野真士，長谷川幸治，北村伸二，山内健一，鳥居行雄，薬科秀紀，岩田　久

【はじめに】

人工股関節再置換術の方法として同種骨を使用したimpaction bone graftingの優れた成績がGieやSlooffらにより報告されている[1,2]．現在，著者らの施設でも人工股関節再置換術にimpaction bone graftingを取り入れ，短期ではあるが良好な成績をおさめている[3,4]．このようにimpaction bone graftingを行う症例，施設の増加に伴い，同種骨移植材料としての大腿骨頭の需要が増加してきている．このため，大腿骨頭を不要とする病院から，必要とする病院への供給システムが必要となってきている．著者らは，大腿骨頭供給システムとしてBone Bank Networkを設立し，その整備に取り組んでいる．

Bone Bank Networkとは図1に示すごとく，基幹病院を中心として各病院と連係をとり，摘出された大腿骨頭を収集，保存，供給するシステムである．

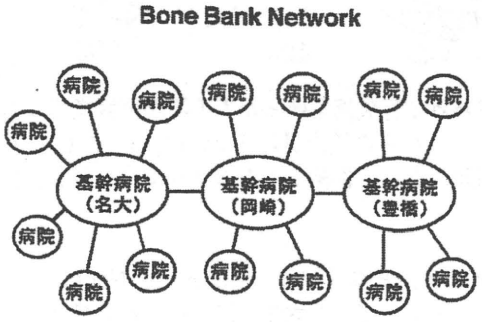

図1

今回，Bone Bank Networkの整備に先立ち，Bone Bank Networkとして供給可能な大腿骨頭数を割り出すこと，Bone Bank Networkを稼動するにあたって問題点を明らかにすることを目的に，名古屋大学整形外科関連病院における同種骨移植状況，大腿骨頭摘出数，術前感染症検査状況を調査検討したので報告する．

【対象および方法】

名古屋大学整形外科の関連68病院に，平成12年4月17日アンケートを郵送し回答を得た．

【結果】

回答病院数56，有効回答率82%であった．回答のあった56病院での大腿骨頚部内側骨折と変股症による年間大腿骨頭摘出総数は1348個であった．同種骨移植を実施している病院は21病院37.5%であり，年間134件の同種骨移植が行われていた（図2）．この21病院中，同種骨を移植前に加温処理していたのは7病院であった．残る14病院の内，放射線照射をしていた1病院を除いた13病院ではまったく処理を行っていなかった．

倫理委員会の有無に関しては有り46%，無し54%と約半数の病院が倫理委員会を設置していた（図3）．摘出した大腿骨頭を保存している病院は22病院，42%あった

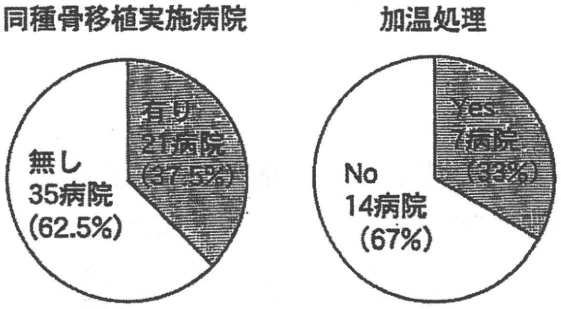

図2

（図4）．このうち32%の病院では倫理委員会の許可を得ていたが，68%では許可を得ていなかった．骨頭を摘出保存している病院で，骨頭提供同意書を使用しているのは32%のみであった（図5）．反対に同種骨移植を行う場合の同種骨移植実施同意書は48%約半数の病院で使用していた．摘出した骨頭の保存温度は95%の病院で-70℃以下で，-70℃以上は1病院だけであった（図6）．骨頭専用の冷凍庫を所有しているのは55%で，残りの45%は検体用の冷凍庫などとの供用であった．

感染症検査に関してはB型肝炎，C型肝炎は100%，梅毒は1病院を除いた全病院で検査していた．しかし，HIVは28病院（55%）の病院でしか検査していなかった．HTLV-1に関してはわずか8病院（16%）で検査しているのみであった（図7）．

Bone Bank Networkへ骨頭提供可能であるかという設問には，25病院（45%）が可能，8病院（14%）が不可能，23病院（41%）が未定であった（図8）．反対にBone Bank Networkからの骨頭を使用可能かという設問に対しては，23病院（41%）が可能，5病院（9%）が不可能，28病院（50%）が未定であった．

以上の結果より，年間大腿骨頭摘出総数からBone Bank Networkに骨頭提供不可能な病院とすでに同種骨移植で骨頭を使用している病院での摘出骨頭数を除くと549個になった．すなわち，この数が計算上ではBone Bank Networkに提供可能だが廃棄されている大腿骨頭数であることがわかった．

【考察】

今回の調査で，名古屋大学整形外科関連病院における同種骨移植状況は，骨頭保存から同種骨移植までquality control, informed consentを含めて各病院様々な方法で行っていることがわかった．このためBone Bank Networkを潤滑に行っていくには日整会ガイドライン[5,6]に乗っ取ったプロトコールの統一が必要であると思われた．このため我々は，Bone Bank Network事務局を設置しBone Bank Networkからプロトコールの提供，保存用バッグの提供，保存バッグ用シールの提供を行うこととした．

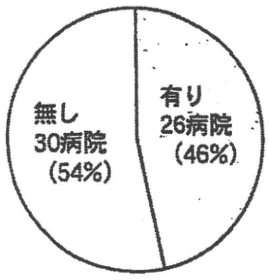

図3

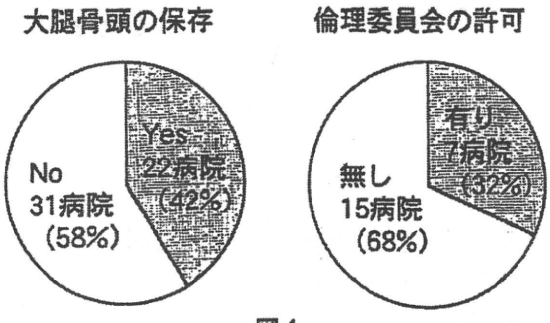

図4

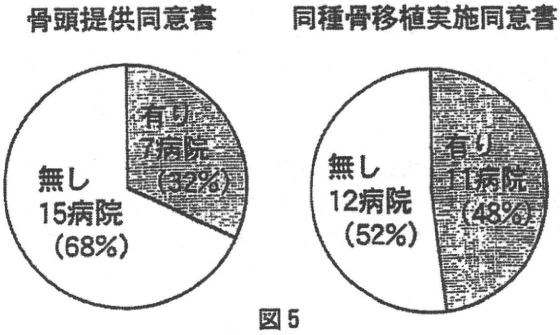

図5

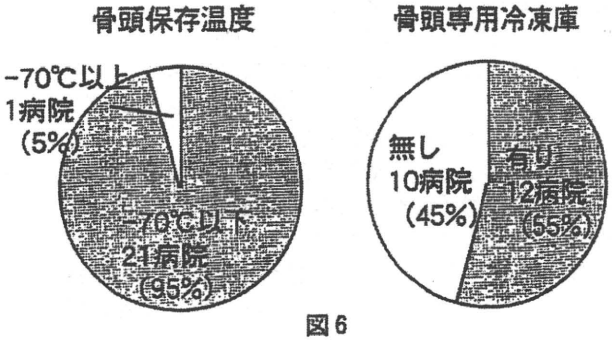

図6

術前あるいは骨頭提供者の感染症検査に関しは，HIV と HTLV-1 は保険点数が認められていないため実施していない病院が多いことがわかった．これに対し，日整会ガイドラインでは同種骨採取にあたり HIV と HTLV-1 検査は必須であるとなっている．同種骨移植を行う場合，disease transmission 防止の観点よりドナーの梅毒，B 型肝炎，C 型肝炎，HIV，HTLV-1 検査は必ず行うべきである．日整会ガイドラインの矛盾を解消するためには，保険行政の改善が必要であると思われた．

現在，利用可能だが廃棄されている大腿骨頭が愛知県内関連病院で年間549個もあることがわかった．今後増加し

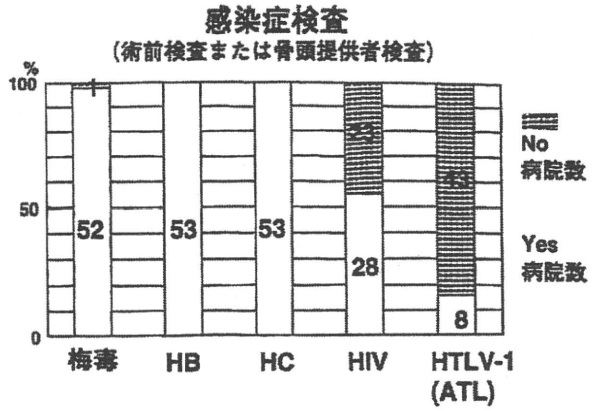

図7

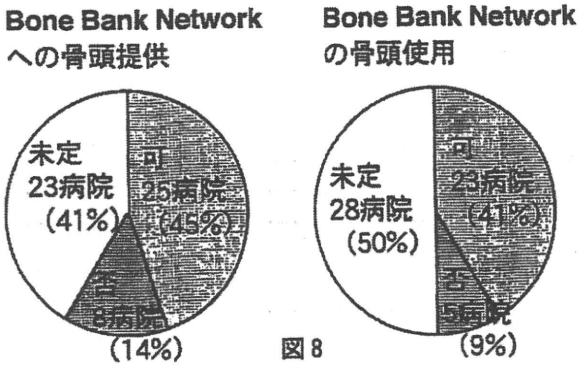

図8

ていくと思われる骨欠損を伴った人工関節再置換術に対応するために，これらの摘出骨頭を quality control のもと有効的に収集，保存，供給するシステムづくりが重要である．

【謝辞】

今回のアンケートならびに Bone Bank Network に協力して下さっている名古屋大学整形外科関連病院と先生方に深謝いたします．

【文献】

1） Gie GA, Linder L, Ling RSM, Simon JP, Slooff TJJH, Timperley AJ: Impacted cancellous allografts and cement for revision total hip arthroplasty. J Bone Joint Surg 75-B: 14-21, 1993.

2） Slooff TJJH, Buma P, Schreurs BW, Schimmel JW, Huiskes R, Gardeniers J. Acetabular and femoral reconstruction with impacted graft and cement. Clin Orthop 1996; 324: 108-15,.

3）坂野真士，長谷川幸治．巨大骨欠損に対する同種骨移植とカップサポーターによる臼蓋再建術．新 OS NOW No.6 新しい人工関節置換術と再置換術．東京：メジカルビュー社；2000：140-6.

4）坂野真士，長谷川幸治，北村伸二，山内健一，岩田久．同種骨移植とカップサポーターによる臼蓋再建術．中部整災誌 43：1251-2, 2000.

5）整形外科移植に関するガイドライン，冷凍ボーンバンクマニュアル，処理骨作製マニュアル（脱脂・凍結乾燥）．日整会誌 1999; 73: 43-70.

6）切除大腿骨頭ボーンバンクマニュアル（生体ドナー）．日整会誌 2000; 74: 52-55.

Kitasato Med J 2011; 41: 76-83

Inactivity but not ovariectomy determines the mechanical property and quality of cortical bone in the hind limbs of aged female rats.

Mitsutoshi Suto,[1] Kouji Naruse,[1] Kentaroo Uchida,[1] Takeaki Yamamoto,[1] Kaori Suto,[1] Ken Urabe,[1] Yuko Mikuni-Takagaki,[2] Moritoshi Itoman[3]

[1] Department of Orthopedic Surgery, Kitasato University School of Medicine
[2] Departments of Functional Biology and Science, Kanagawa Dental College
[3] Kyushu Rosai Hospital

Objective: Our goal in this study was to determine the physiological consequences of ovariectomy (OVX) and a lack of daily activity such as walking.
Methods: We forced 40-week-old female rats to be inactive for 13 weeks with an experimental system that prevents standing and walking while allowing other movements. Rats were either ovariectomized or underwent a sham operation at 40 weeks and then were maintained for 13 weeks individually in standard cages or in cages with limited space. Tibiae and femora were analyzed by pQCT (peripheral quantitative computed tomography), micro-CT (microfocused x-ray computed tomography), Raman spectroscopy, and the three-point bending test.
Results: Significant bone loss occurred only by OVX and was limited to the cancellous bone compartment. Cortical bone was affected by the forced inactivity but not by OVX, and the breaking force of inactive rat femur was lower than that of the walking rats.
Conclusions: It is concluded that the lack of daily activity is detrimental to the strength and quality of bone, while lack of estrogen mainly affects the cancellous bone properties.

Key words: physical activity, cortical bone, osteoporosis, Raman spectroscopy, quality of bone

Introduction

Bone changes by age, hormonal status, diseases, and mechanical environment. Among the methods employed to study bones, bone marrow density (BMD) had been widely used as a measure of bone health. Evidence suggests, however, that the quality of cortical bone should also be taken into account when assessing bone strength, as well as the fracture risk.[1,2] Structure (geometry) and the material properties, namely the quality, can be assessed noninvasively by peripheral quantitative computed tomography (pQCT) and infrared/Raman vibrational spectroscopy.[3,4] By confocal laser Raman spectroscopy, we analyzed the extent of matrix mineralization (mineral/matrix ratio) and the characteristics of hydroxyapatite and collagen including the CO_3/PO_4 ratio, the crystallinity, and the extent of proline hydroxylation that leads to the formation of mature cross-links.[5,6] We studied these parameters in the cortical bone of aged female rats, whose physical activity was restricted or they were ovariectomized. We controlled physical activity by keeping the experimental rats in special cages that forced them to be inactive.[6]

While ovariectomized (OVX)-rats have provided an excellent animal model for postmenopausal osteoporosis for more than a quarter century,[7,8] no adequate rat models have been available to test the effect of an inactive lifestyle. Studies have been limited to rodent models in which legs are locally immobilized, as in hindlimb unloading, in which case periosteal bone formation decreases. Significant changes in the major parameters of bone, such as the mechanical properties, BMD, and bone mineral content BMC, occur only when the two interventions, unloading and ovariectomy, are combined.[9,10] We, therefore, sought to characterize the effect of estrogen deprivation and lack of physical activity separately on the hindlimb bones of aged female rats with our caged-rat model, in which the cage prevents rats from standing or walking while allowing other movements.

Received 15 November 2010, accepted 22 November 2010
Correspondence to: Kouji Naruse, Department of Orthopedic Surgery, Kitasato University School of Medicine
1-15-1 Kitasato, Minami-ku, Sagamihara, Kanagawa 252-0374, Japan
E-mail: knaruse@med.kitasato-u.ac.jp

Materials and Methods

Animals and experimental design

The protocol for the experiment was approved by the animal care committee of Kitasato University School of Medicine. Female Wistar rats, purchased from Charles River Japan, Inc., were maintained at the animal facility of Kitasato University with rodent Diet CE-2 (CLEA Japan, Inc.), which contains 1.18 g calcium and 1.03 g phosphorus in 100 g of feed. Rats were either the OVX group or underwent a sham operation at 40 weeks, and then were maintained for 13 weeks individually in standard cages (the Sham group) or in cages with limited space, 70 mm × 180 mm × 53-130 mm (W × L × H) (the Res group). The animals were pair-fed by the method used by Scarpace et al. with a minor modification.[6,11] All rats were killed, and the femurs and tibiae were excised and stored at -80℃ until being tested biomechanically. Alternatively, the excised legs were fixed with 4% paraformaldehyde for 48 hours and then replaced with PBS (phosphate buffer saline) for micro-CT and pQCT analyses.

Micro-CT

A micro-CT equipped with a microfocus x-ray tube (focus size 8 × 8 μm, inspeXio SMX-90CT Shimadzu Corporation, Tokyo) was used to obtain images of an area in tibia starting 500 μ m from the most distal part of the growth plate and extending 3 mm distally. The tube voltage, tube current, magnification, and voxel size were 90 kV, 110 μA, × 7, and 13.0 × 13.0 × 13.0 μm, respectively. Using TRI/3D BON software (Ratoc System Engineering Co., Ltd, Tokyo), 3D structural parameters, such as bone volume fraction, BV/TV (%), BMC (mg), BMD (mg/cm^3), trabecular thickness (Tb.Th μm), trabecular number (Tb.N 1/mm), and trabecular separation (Tb.Sp μm) were calculated.[6]

pQCT analysis

For the pQCT analysis, isolated bones were measured using an XCT Research SA+ pQCT instrument (Stratec Medizintechnik GmbH, Pforzheim, Germany) with a tube voltage of 50 kV and a tube current of 550 μA using a voxel size of 80 × 80 × 460 μm. Cortical bone was defined as the voxels of bone with BMD greater than 690 mg/cm^3. Trabecular bone was defined as voxels of bone with BMD less than 395 mg/cm^3.[3] Femur slices at 15 mm from the distal end were used for cortical BMD measurements. Cross-sectional moment of inertia (CSMI) was calculated on the frontal plane as reported.[6]

Mechanical testing

The mechanical properties of the right femora were measured using the three-point bending method and an MZ-500S mechanical testing device (Maruto Co., LTD., Tokyo). The bending load was applied at 15 mm from the distal end of the femur on the anterior surface at a speed of 10 mm/minute until fracture was made, with the posterior surface of the femur face down on supports 17 mm apart. The ultimate force, breaking force, stiffness (slope of the load-displacement curve), and work-to-failure (area under the load-displacement curve before the fracture occurs) were measured as whole-bone mechanical properties.

Confocal laser Raman spectroscopic measurements

Confocal laser Raman microspectroscopy was used to determine the composition and relative intensities of mineral and matrix in the mid-shaft anterior cortex of the left femur 15 mm from the distal end. Intracortical compartment was subjected to measurements by a Nicolet Almega XR Dispersive Raman microscope system equipped with the OMNIC Atlus imaging software program (ThermoFisher Scientific, Inc., MA, USA). An area less than 1 μm^3 can be mapped using Atlus mapping with a visualized sample on the video microscope. A high-brightness, low-intensity laser operating at 780 nm was used as the excitation source with a laser power of 35 mW. Each spectrum is the sum of 10 10-second measurements. The peak areas were calculated between the following Raman shift numbers: $PO4^{3-}v_1$, 981.9-925.7 cm^{-1}; $PO_4^{3-}v_4$, 631.0-545.8 cm^{-1}; $CO_3^{2-}v_1$, 1087.9-1052.1 cm^{-1}; amide I, 1716.3-1541.2 cm^{-1}; amide III, 1298.1-1214.4 cm^{-1}; hydroxyproline, 855 and 878 cm^{-1}; proline, 919 cm^{-1}; as in Akkus et al.[12] Mature collagen cross-links were determined as the ratio of the peak heights at 1,660 cm^{-1} and 1,690 cm^{-1}, which correspond to pyridinoline [Pyd] cross-link and dehydrodihydroxylysinonorleucine [deH-DHLNL]), respectively. Crystallinity, parameter of mineral maturation, was determined as the inverse of the width of the phosphate symmetric-stretch band ($PO_4^{3-}v_1$ at 959 cm^{-1}) at half the maximum intensity value.[13]

Statistic analysis

All data values are expressed as the mean ± standard deviation (SD). The group means were compared by one-way analysis of variance (ANOVA) followed by Tukey's multiple comparison test using a commercially available statistical package (SPSS 11.0 J for windows, SPSS Japan).

Table 1. Body weight and lower limb bone length

Parameters	Treatment		
	Sham (n = 10)	OVX (n = 9)	Res (n = 10)
Age (weeks)	53	53	53
Body weight (g)	408.2 ± 49.0	437.3 ± 34.8	387.9 ± 28.4
Femur length (mm)	37.1 ± 0.8	37.7 ± 1.1	37.3 ± 0.6
Tibia length (mm)	40.1 ± 1.0	40.2 ± 1.4	40.2 ± 0.4

No significant differences were detected among the groups.

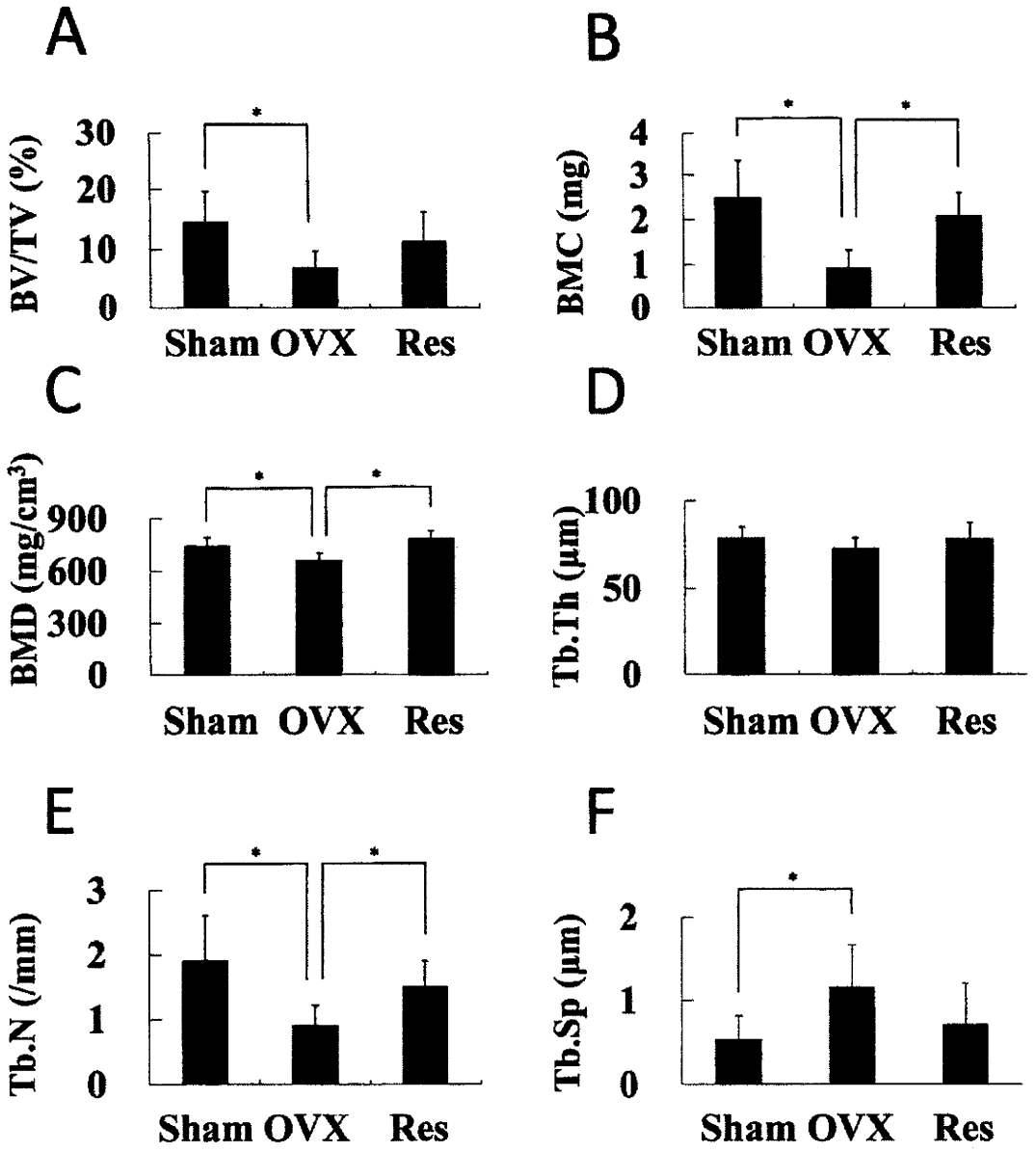

Figure 1. Effect of inactivity or ovariectomy on micro-CT parameters of femoral cancellous bone in the Sham, OVX, and Res groups.

(**A**) Bone volume fraction, BV/TV (%), (**B**) bone mineral content, BMC (mg) and (**C**) density, BMD (mg/cm³), (**D**) trabecular thickness, Tb.Th (μm), (**E**) number Tb.N (1/mm), and (**F**) separation, Tb.Sp (μm), are shown. The group means for each parameter were compared using a one-way analysis of variance (ANOVA) followed by Tukey's multiple comparison test. Bars represent the means ± SD. Asterisks above connected pairs of values indicate significant differences (*$P < 0.05$).

Results

Final body weight and lower-limb bone lengths

Measurements at the time of sacrifice were summarized in Table 1. While there was a trend of lighter body weight in the Res group than in the walking groups (Res < Sham < OVX, without significance), no intergroup differences were detected.

Micro-CT analysis of BMD and trabecular morphology in tibia epiphysis

Parameters of trabecular bone in the proximal tibia showed that ovariectomy caused significant bone loss in the OVX group; in BV/TV and Tb.Sp compared with the Sham group; and in BMD, BMC, and Tb.N, compared with both the Sham and Res groups (Figure 1). Tb.Th was unchanged in all the treatments.

Table 2. Cortical bone parameters by pQCT analysis of femur diaphysis

Parameters	Treatment		
	Sham (n = 10)	OVX (n = 9)	Res (n = 10)
Cortical BMD (mg/cm^3)	1,392.5 ± 10.9	1,375.6 ± 30.4	1,395.5 ± 18.8
Cortical BMC (mg)	9.5 ± 0.6	9.3 ± 0.5	9.3 ± 0.6
Cortical area (mm^2)	6.8 ± 0.4	6.8 ± 0.4	6.7 ± 0.5
Pericortical perimeter (mm)	15.3 ± 0.8	15.6 ± 0.8	15.3 ± 0.6
Endocortical perimeter (mm)	11.9 ± 0.9	12.1 ± 0.9	11.8 ± 0.8
x-Axis SSI (mm^3)	4.7 ± 0.7	4.6 ± 0.5	4.6 ± 0.6

No significant differences were detected among the groups.

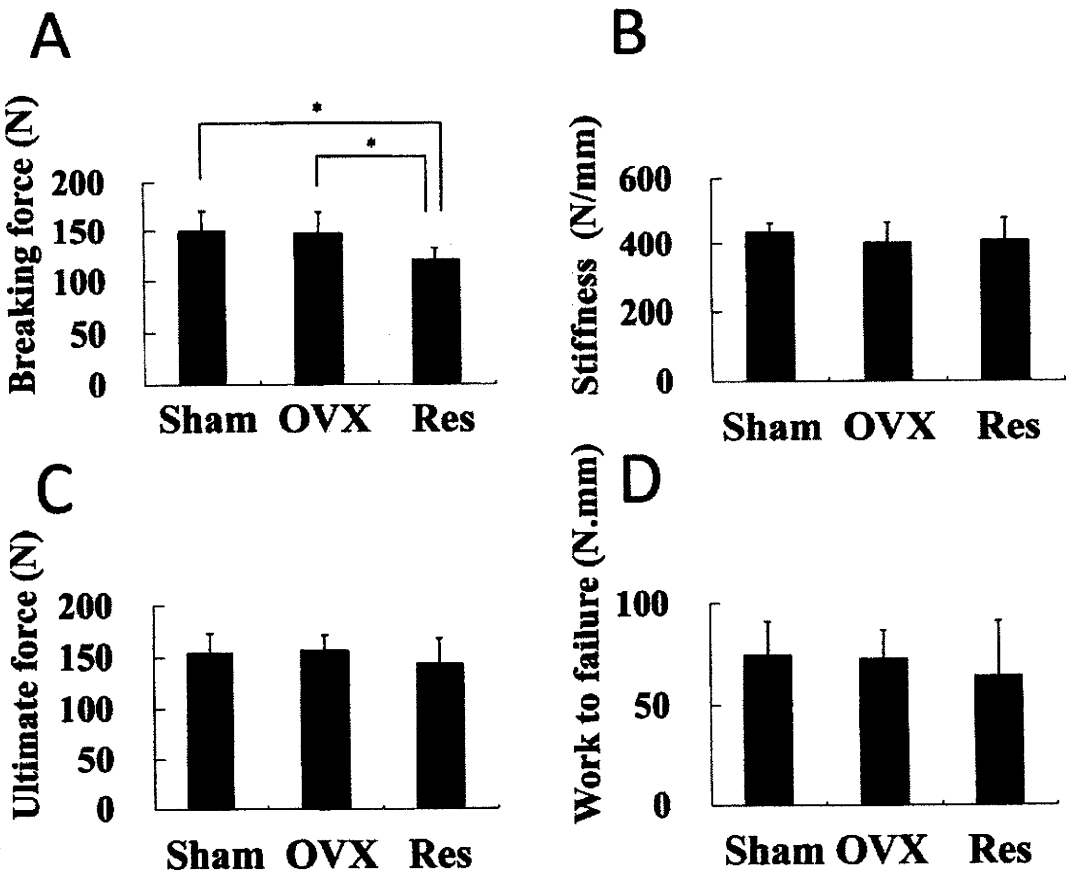

Figure 2. Effect of inactivity or ovariectomy on mechanical properties of femur. The whole-bone mechanical properties measured are (**A**) breaking force, (**B**) stiffness (slope of the load-displacement curve), (**C**) ultimate force, and (**D**) work-to-failure (area under the load-displacement curve before fracture). Only the breaking force showed significant difference among the Sham and Res and OVX groups. Bars and significance are as in Figure 1.

Cortical parameters of BMD and geometry determined by pQCT analysis

The cortical BMD values in femur at the mid-shaft were almost identical among the three groups (Table 2). In addition, no intergroup differences were detected in cortical BMC, cortical area, pericortical perimeter, endcortical perimeter, or x-axis CSMI.

Mechanical properties

Figure 2 shows the mechanical measurements of the femur by the three-point bending test. The breaking force value in the Res group was significantly lower than that of the Sham and OVX groups. Regarding ultimate force, stiffness, and work-to-failure, we found only a trend with no significant difference between the groups.

Confocal laser Raman spectroscopic measurements of material properties

An analysis of the anterior cortex of the femurs revealed the resolvable mineral factor was carbonated apatite. The peak wave numbers were almost identical to those originally reported by Tarnowski et al.[14] as shown in Figure 3A. Figure 3B-I summarizes the results. The carbonate to phosphate ratio as well as the crystallinity in the OVX and Res groups is not significantly different from those in the Sham group. In the collagenous matrix, however, both the hypro/pro ratio and the mature collagen cross-link values were significantly lower in the Res group than in the Sham group, showing that collagen in the inactive rat bone is not properly processed after translation/secretion. Moreover, the mineral-to-matrix ratio, the relative peak areas of $PO_4^{3-}v_1$ to amide I and $PO_4^{3-}v_4$ to amide III, significantly increased in the Res group (vs. those in the Sham group). From the original Raman intensity (Figure 3H and I), it is apparent that Amide III is much less in the Res bone matrix than that in the Sham bone matrix.

Discussion

Although postmenopausal estrogen loss is an essential factor in the pathogenesis of osteoporosis in elderly women, there is, to date, no proper measure to estimate how the lack of physical activity contributes to this pathogenesis. Therefore, it will be beneficial to identify the two components experimentally in order to better understand and treat postmenopausal osteoporosis. Our model is intended to mimic the conditions of elderly women who walk less than a mile a week, whose bone is inferior to that of walking women.[15] Our data showed that inactivity but not ovariectomy causes local weakening of cortical bone material properties.

Entirely different results from our inactive rat model have been reported in most disuse models including the hindlimb unloading rodent model.[16] In rapid endocortical bone loss in hindlimb-unloaded mice, sympathetic nervous tone mediates an unloading-induced 40%-60% loss of trabecular bone volume per trabecular volume (BV/TV) in 10 days, which acts through suppression of bone formation by osteoblasts and enhancement of resorption by osteoclasts.[17] In 6-month-old rats, Tou et al. reported that neither single intervention, hindlimb

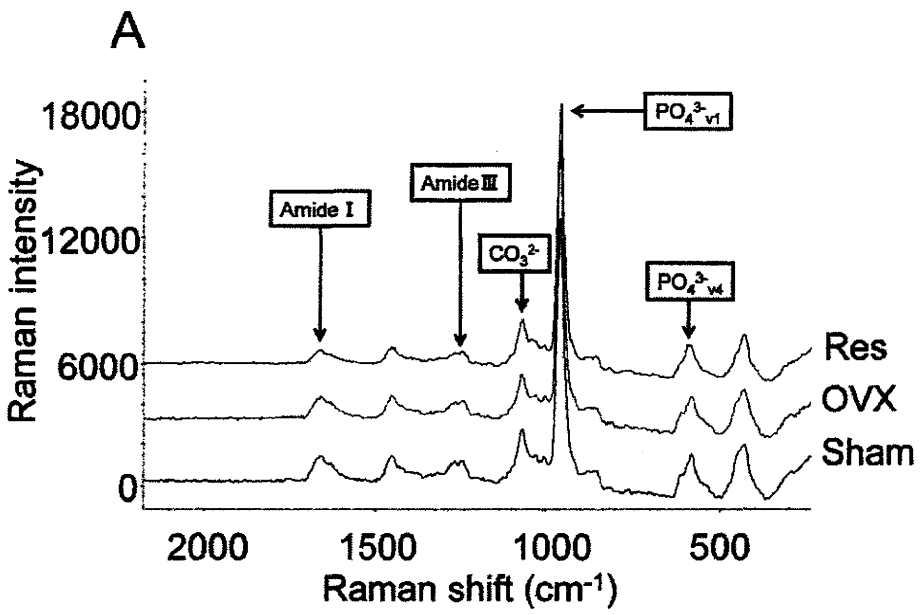

Figure 3. (Continued on the following page)

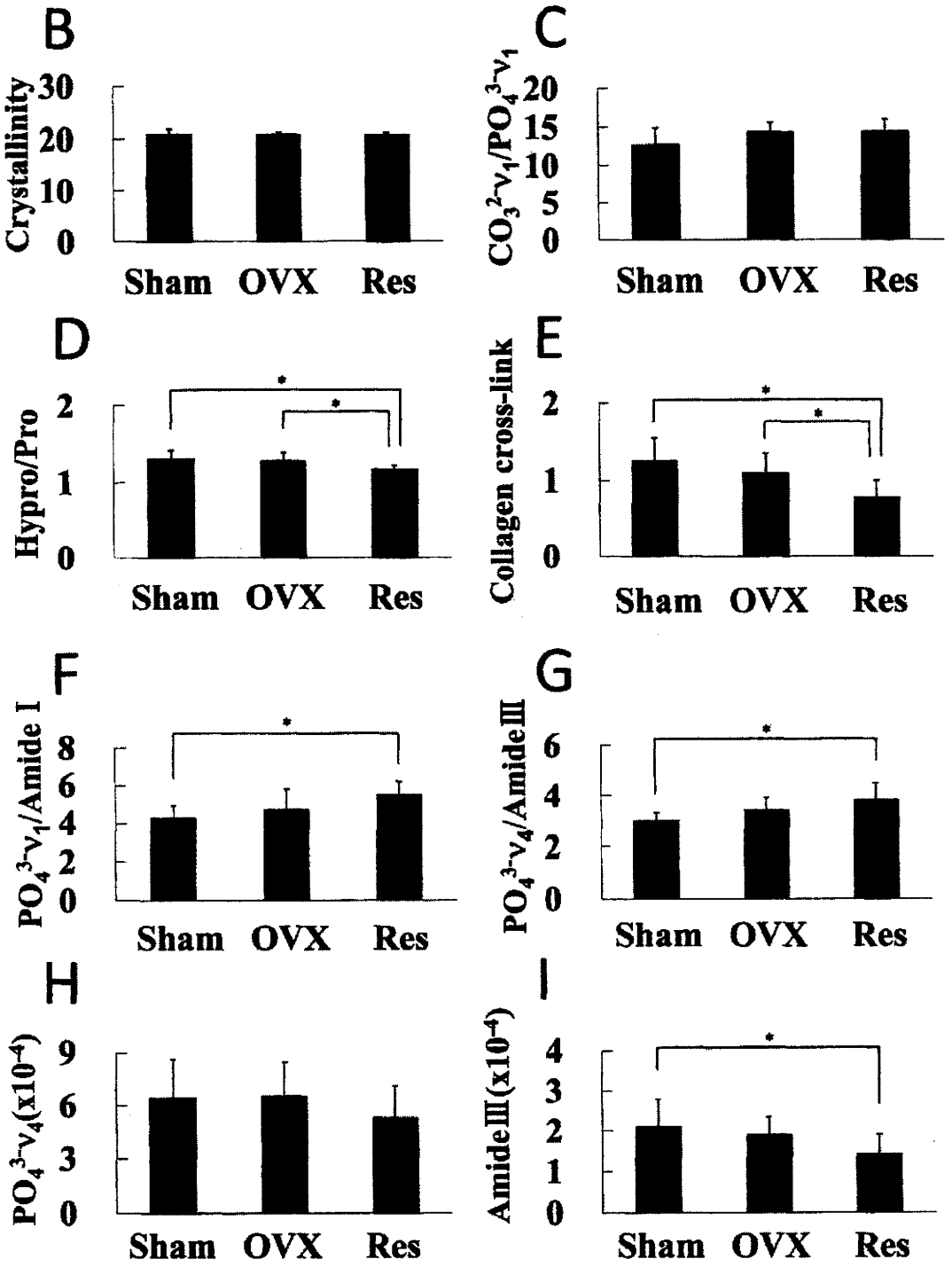

Figure 3. (Continued from the previous page) Effect of inactivity or ovariectomy on mineral and matrix parameters analyzed by intracortical measurements of bone components by confocal laser Raman vibrational spectroscopy. (A) Representative spectra from the three groups, Sham control, OVX and Res, (B) crystallinity, ratios of (C) $CO_3^{2-}/PO_4^{3-}\nu_1$, (D) Hypro/Pro, (E) Pyd/ deH-DHLNL, (F) $PO_4^{3-}\nu_1$/amide I and (G) $PO_4^{3-}\nu_4$/ amide III, and peak intensities of $PO_4^{3-}\nu_4$ and amide III are shown. Bars and significance are as in Figure 1.

unloading or OVX, reduced bone strength as revealed by torsion tests and that there was a correlation between lower femoral total BMD ($r2 = 0.65$, $P < 0.001$) and reduced torque strength with the combined intervention.[10] These results suggest that the restricted movement resulted in underuse, which is distinct from disuse in that only the quality of bone severely changes. Collagen cross-linking chemistry was discussed as a function of age.[18-20] A likely consequence of aging, we believe, is underuse and underloading of bone.

We have detected no significant difference in the intensity of mineral parameters by Raman microspectroscopy. On the other hand, lower matrix intensity derived not only from >C = O vibration (Amide I and Amide III) but also from $>CH_2$ vibration (data not shown). The significantly higher mineral/matrix content, therefore, likely derives from the lower collagen content in the inactive rat cortex than in that of walking rats. Comparing the inbred strains of mice, Courtland et al. reported that A/J mouse femora had a higher mineral/matrix ratio than C57BL/6J (B6) femora, which demonstrated significantly higher work-to-failure and toughness values than A/J femora.[21] Although not significant, work-to-failure values are lower in the Res rat femora than in other groups suggesting a similar brittleness of cortical bone in the inactive rats.

We propose that daily activity, such as walking, is a determinant of the properties of cortical bone. Our inactive rat model will be useful in the future studies of anabolic drugs, which counteract disuse osteoporosis.[22,23]

Acknowledgments

We thank Shimada C, Ueno M, Ohashi M, Kuranaga M, Kashima I, and Kozai Y for their technical assistance and Dr. Yamato H for his helpful suggestions.

This investigation was supported in part by a research grant from the Parents' Association of Kitasato University School of Medicine and Postgraduate Research project No.2010-B06 at the Graduate School of Medical Science, Kitasato University to MS and by grants-in-aid from the Ministry of Science, Education, and Culture of Japan to KN and YM-T.

References

1. Burr DB. Bone material properties and mineral matrix contributions to fracture risk or age in women and men. *J Musculoskelet Neuronal Interact* 2002; 2: 201-4.
2. Wang X, Shen X, Li X, et al. Age-related changes in the collagen network and toughness of bone. *Bone* 2002; 31: 1-7.
3. Ferretti JL. Peripheral quantitative computed tomography (pQCT) for evaluating structural and mechanical properties of small bone. In: An YH, Draughn RA, editors. Mechanical testing of bone and the bone-implant interface. Boca Raton: CRC Press; 1999; 385-405.
4. Gourion-Arsiquaud S, Boskey AL. Fourier transform infrared and Raman microspectroscopy and microscopic imaging of bone. *Curr Opin Orthop* 2007; 18: 499-504.
5. Matsumoto Y, Mikuni-Takagaki Y, Kozai Y, et al. Prior treatment with vitamin K(2) significantly improves the efficacy of risedronate. *Osteoporos Int* 2009; 20: 1863-72.
6. Miyagawa K, Kozai Y, Ito Y, et al. A novel underuse model shows that inactivity but not ovariectomy determines the deteriorated material properties and geometry of cortical bone in the tibia of adult rats. *J Bone Miner Metab* 2010 Dec 3 [Epub ahead of print] (in press).
7. Hori M, Takahashi H, Konno T, et al. Effect of elcatonin on experimental osteoporosis induced by ovariectomy and low calcium diet in beagles. *Nippon Yakurigaku Zasshi* 1984; 84: 91-8.
8. Kalu DN. Evaluation of the pathogenesis of skeletal changes in ovariectomized rats. *Endocrinology* 1984; 115: 507-12.
9. Bagi CM, Mecham M, Weiss J, et al. Comparative morphometric changes in rat cortical bone following ovariectomy and/or immobilization. *Bone* 1993; 14: 877-83.
10. Tou JC, Foley A, Yuan YV, et al. The effect of ovariectomy combined with hindlimb unloading and reloading on the long bones of mature Sprague-Dawley rats. *Menopause* 2008; 15: 494-502.
11. Scarpace PJ, Matheny M, Moore RL, et al. Impaired leptin responsiveness in aged rats. *Diabetes* 2000; 49: 431-5.
12. Akkus O, Adar F, Schaffler MB. Age-related changes in physicochemical properties of mineral crystals are related to impaired mechanical function of cortical bone. *Bone* 2004; 34: 443-53.
13. Yerramshetty JS, Lind C, Akkus O. The compositional and physicochemical homogeneity of male femoral cortex increases after the sixth decade. *Bone* 2006; 39: 1236-43.
14. Tarnowski CP, Ignelzi MA Jr., Morris MD. Mineralization of developing mouse calvaria as revealed by Raman microspectroscopy. *J Bone Miner Res* 2002; 17: 1118-26.
15. Krall EA, Dawson-Hughes B. Walking is related to bone density and rates of bone loss. *Am J Med* 1994; 96: 20-6.

16. Jee WS, Ma Y. Animal models of immobilization osteopenia. *Morphologie* 1999; 83: 25-34.
17. Kondo H, Nifuji A, Takeda S, et al. Unloading induces osteoblastic cell suppression and osteoclastic cell activation to lead to bone loss via sympathetic nervous system. *J Biol Chem* 2005; 280: 30192-200.
18. Eyre DR, Dickson IR, Van Ness K. Collagen cross-linking in human bone and articular cartilage. Age-related changes in the content of mature hydroxypyridinium residues. *Biochem J* 1988; 252: 495-500.
19. Fujii K, Kuboki Y, Sasaki S. Aging of human bone and articular cartilage collagen: changes in the reducible cross-links and their precursors. *Gerontology* 1976; 22: 363-70.
20. Saito M, Marumo K, Fujii K, et al. Single-column high-performance liquid chromatographic-fluorescence detection of immature, mature, and senescent cross-links of collagen. *Anal Biochem* 1997; 253: 26-32.
21. Courtland HW, Nasser P, Goldstone AB, et al. Fourier transform infrared imaging microspectroscopy and tissue-level mechanical testing reveal intraspecies variation in mouse bone mineral and matrix composition. *Calcif Tissue Int* 2008; 83: 342-53.
22. Ma Y, Jee WS, Yuan Z, et al. Parathyroid hormone and mechanical usage have a synergistic effect in rat tibial diaphyseal cortical bone. *J Bone Miner Res* 1999; 14: 439-48.
23. Tian X, Jee WS, Li X, et al. Sclerostin antibody increases bone mass by stimulating bone formation and inhibiting bone resorption in a hindlimb-immobilization rat model. *Bone* 2011; 48: 197-201.

Cell Tissue Bank
DOI 10.1007/s10561-010-9234-0

ORIGINAL PAPER

Repeated freeze–thaw cycles reduce the survival rate of osteocytes in bone-tendon constructs without affecting the mechanical properties of tendons

Kaori Suto · Ken Urabe · Kouji Naruse · Kentaro Uchida · Terumasa Matsuura · Yuko Mikuni-Takagaki · Mitsutoshi Suto · Noriko Nemoto · Kentaro Kamiya · Moritoshi Itoman

Received: 6 August 2010 / Accepted: 18 November 2010

Abstract Frozen bone-patellar tendon bone allografts are useful in anterior cruciate ligament reconstruction as the freezing procedure kills tissue cells, thereby reducing immunogenicity of the grafts. However, a small portion of cells in human femoral heads treated by standard bone-bank freezing procedures survive, thus limiting the effectiveness of allografts. Here, we characterized the survival rates and mechanisms of cells isolated from rat bones and tendons that were subjected to freeze–thaw treatments, and evaluated the influence of these treatments on the mechanical properties of tendons. After a single freeze–thaw cycle, most cells isolated from frozen bone appeared morphologically as osteocytes and expressed both osteoblast- and osteocyte-related genes. Transmission electron microscopic observation of frozen cells using freeze-substitution revealed that a small number of osteocytes maintained large nuclei with intact double membranes, indicating that these osteocytes in bone matrix were resistant to ice crystal formation. We found that tendon cells were completely killed by a single freeze–thaw cycle, whereas bone cells exhibited a relatively high survival rate, although survival was significantly reduced after three freeze–thaw cycles. In patella tendons, the ultimate stress, Young's modulus, and strain at failure showed no significant differences between untreated tendons and those subjected to five freeze–thaw cycles. In conclusion, we identified that cells surviving after freeze–thaw treatment of rat bones were predominantly osteocytes. We propose that repeated freeze–thaw cycles could be applied for processing bone-tendon constructs prior to grafting as the treatment did not affect the mechanical property of tendons and drastically reduced surviving osteocytes, thereby potentially decreasing allograft immunogenecity.

Keywords Allografts · Freeze-thawing · Bone-patellar tendon-bone · Osteocytes

K. Suto · K. Urabe (✉) · K. Naruse · K. Uchida · T. Matsuura · M. Suto
Department of Orthopaedic Surgery, Kitasato University School of Medicine, 1-15-1 Kitasato, Minami-ku, Sagamihara, Kanagawa 252-0374, Japan
e-mail: kenurabe@med.kitasato-u.ac.jp

Y. Mikuni-Takagaki
Department of Science, Kanagawa Dental College, 82 Inaokacho, Yokosuka, Kanagawa 238-8580, Japan

N. Nemoto
Research Center for Biological Imaging, Kitasato University School of Medicine, 1-15-1 Kitasato, Minami-ku, Sagamihara, Kanagawa 252-0374, Japan

K. Kamiya
Rehabilitation Center, Kitasato University Hospital, 1-15-1 Kitasato, Minami-ku, Sagamihara, Kanagawa 252-0375, Japan

M. Itoman
Kyushu Rosai Hospital, 1-3-1 Kuzuhara-Takamatsu, Kokura-Minami, Kitakyushu, Fukuoka 800-0296, Japan

Published online: 30 November 2010

Introduction

Of the knee ligaments, the anterior cruciate ligament (ACL) is most prone to total disruption, which is often followed by repeated episodes of joint instability associated with meniscal injury, increased erosion of joint cartilage, and abnormal osseous metabolic activity (Beynnon et al. 2002). Conservative management of ACL deficiency leads to progressive rotatory instability, meniscal tears, and premature joint degeneration (Barrett 1991). To restore rotatory stability, reconstruction of the ACL is typically performed by a variety of grafting procedures using autografts, allografts, or artificial ligaments. Although autografts are nonimmunogenic and therefore represent a good alternative for the replacement of missing ligaments, allografts have many advantages over autografts, including a lack of donor site morbidity, shorter operation time, and larger grafts are possible (Kleipool et al. 1998). Despite these benefits, viable cells present in allografts are capable of eliciting host immune responses that reduce the effectiveness of ACL reconstruction, and it is unclear what cell types are responsible for the immunoreactivity.

Allografts are transplanted after they are subjected to various processes for reducing antigenicity, sterilization, and preservation. Freezing of tissues at −80°C is generally used for long storage in tissue banks and is also considered to reduce immunogenicity of allografts as tissue cells are killed (Gitelis and Cole 2002; Weyts et al. 2003; Heyligers and Klein-Nulend 2005); however, recent studies have reported that a small portion of bone cells survive in human resected femoral heads after standard bone-bank freezing protocols (Weyts et al. 2003; Heyligers and Klein-Nulend 2005; Simpson et al. 2007). As the detailed characterization of surviving cells in allografts has not been performed, it is important to identify surviving cell types and survival mechanisms during freezing procedures to more effectively target these cells and improve the success of allograft procedures.

During the freezing process, cells undergo injury due to intracellular ice crystal formation and the altered ionic concentrations of solutions (Gage and Baust 1998). Repeated freeze–thaw cycles result in greater tissue destruction than a single freeze–thaw cycle (Gill et al. 1968), due in large part to an increase in cell necrosis (Dilley et al. 1993). We therefore hypothesized that repeated freeze–thaw cycles would reduce the number of surviving cells in allografts, and potentially represents a simple method for reducing immunogenicity. Although we previously reported that a single freeze–thaw cycle did not affect the mechanical properties of tendons (Park et al. 2009), it is unclear how repeated freeze–thaw treatments would affect tendon mechanics and function.

The purpose of this study was to characterize the survival rate and mechanisms of cells from rat bones and tendons that were subjected to repeated freeze–thaw treatments, and evaluate the influence of these treatments on the mechanical properties of tendons.

Materials and methods

Bone preparation

Long bones (femora and tibiae) were harvested from 10-week-old male Wistar rats (Charles River Japan, Yokohama, Japan). Bones from 16 rats were divided into four freeze–thaw (FT) groups: (a) FT0, in which bones were fresh; (b) FT1, in which bones were frozen using an ultra-low temperature freezer (MDF-U581, Sanyo Electric Co., Ltd, Osaka, Japan) and stored at −80°C for 3 weeks; (c) FT2, in which FT1 were thawed at 37°C in for 1 h, and then stored at −80°C for 1 week; and (d) FT3, in which FT2 were subjected to a third thawing and freezing cycle and then stored at −80°C for 1 week.

Isolation and culture of bone cells

For the isolation and culture of bone cells from the FT1 group, frozen bone samples were first thawed at room temperature in a phosphate-buffered saline without Mg^{2+} and Ca^{2+} (PBS(−)). Bone samples, including cartilage, were collected by chipping femora and tibiae with scissors. Pieces of bones were then digested twice with collagenase (Wako Pure Chemical Industries, Ltd., Osaka, Japan) in PBS containing Mg^{2+} and Ca^{2+} (PBS(+)) at 37°C on a rotary blood mixer for 15 min, as previously described (Mikuni-Takagaki et al. 1995), and a single fraction (Fr) was collected after each digestion to yield Fr 1 and 2. Subsequently, pieces of bones were then consecutively digested three times with

collagenase for 20 min, and osteoblastic populations were obtained from each collagenase solution to give Fr 3, 4, and 5. After the collection of Fr 5, osteocyte-rich populations were obtained from the remaining cells by an initial incubation in PBS(−) containing 4 mM EDTA for 15 min to yield Fr 6-1, followed by a 15-min incubation in a collagenase solution for 15 min to give Fr 6-2. This procedure was repeated to yield Fr 7-1 and 7-2. Following the final digestion, cell suspensions were sequentially passed through 100 and 40 μm filters and then cultured in type I collagen-coated culture dishes with alpha-minimum essential medium (α-MEM) supplemented with 5% fetal bovine serum (FBS), 5% calf serum (CS), 0.25 mM ascorbic acid, 100 units/ml penicillin, and 100 μg/ml streptomycin for 1 week at 37°C in a humidified atmosphere containing 5% CO_2 (MCO-20AIC, Sanyo Electric Co., Ltd., Osaka, Japan). Adherent bone cells were then observed by phase-contrast microscopy (ECLIPSE TS100, Nikon, Tokyo, Japan) and cell survival frequency (frequency of at least one cell surviving) was then calculated.

Isolation and culture of tendon cells

Patellar tendons (PTs) were collected from both knees of 15 10-week-old male Wistar rats after being freed from surrounding tissues using sharp scissors. The harvested PTs were divided into an FT0 group, which consisted of fresh PTs, and an FT1 group, which consisted of PTs that were frozen using an ultra-low temperature freezer, stored at −80°C for 3 weeks, and then thawed at room temperature in PBS(−). Tendon cells were harvested by collagenase digestion, as previously described (Scutt et al. 2008). Briefly, PTs were rinsed once in PBS(−), diced into small pieces, and then digested in a sterile collagenase solution for either 4, 8, or 18 h at 37°C on a rotary blood mixer at 180 rpm. Following digestion, cell suspensions were sequentially passed through 100 and 40 μm filters, and then cultured in culture dishes with Dulbecco's Modified Eagle Medium (D-MEM) containing 10% FBS, 50 μg/ml ascorbic acid, 100 units/ml penicillin, and 100 μg/ml streptomycin. After 1 week, PT-derived adherent cells were observed by phase-contrast microscopy and cell survival rate was calculated.

Reverse transcription-polymerase chain reaction (RT–PCR)

To determine the characteristics of surviving cells, cell marker gene expression was analyzed by RT–PCR. Total cellular RNA was first extracted with Trizol Reagent (Invitrogen, Carlsbad, USA) according to the manufacturer's instructions. To generate cDNA from total RNA, reverse transcription was performed using SuperScript™ II Reverse Transcriptase (Invitrogen, Carlsbad, USA) (Naruse et al. 2000; Uchida et al. 2007). Expression of the osteoblast-related marker genes alkaline phosphatase (ALP), parathyroid hormone receptor (PTHr), alpha-1 type I collagen (COL1A1), and osteocalcin (OCN) and the osteocyte-related marker genes sclerostin (SOST) and dentin matrix protein-1 (DMP-1) in Fr 5–7 was analyzed by RT–PCR. Newly designed primers were used to amplify OCN, SOST, and DMP-1 (Table 1), and primers designed based on previously published cDNA sequences (Naruse et al. 2004; Uchida et al. 2007) were used for all other target genes. All primers were purchased from Sigma Genosys (Hokkaido, Japan).

Table 1 Primer pairs used for PCR amplification

Target gene	Accession no.[a]	Primer pair sequences (sense/antisense)[b]	Base pairs	Cycles
OCN	X04141	5′-TGAGGACCCTCTCTCTGCTC-3′	127	30
		5′-ACCTTACTGCCCTCCTGCTT-3′		
SOST	AF326741	5′-CAGCTCTCACTAGCCCCTTG-3′	228	30
		5′-CTCGGACACGTCTTTGGTGT-3′		
DMP-1	NM_203493	5′-AGTTCGATGATGAGGGGATG-3′	299	30
		5′-AGTCTCGCTCCTGCTTTCCT-3′		

OCN Osteocalcin, *SOST* sclerostin, *DMP-1* dentin matrix protein-1

[a] Genbank accession number of the sequences used in designing the primers

[b] Primer sequences were designed using BLUEPHIN software (Sigma Genosys, Japan)

RT–PCR was performed under linear conditions, and the following conditions were used for the amplification of all genes: an initial denaturation for 5 min at 94°C, followed by a cycle of denaturation at 94°C for 30 s, a specific annealing temperature (55–60°C) for each pair of primers for 30 s, extension at 72°C for 30 s, followed by a final elongation step of 2 min at 72°C. Amplified PCR products were separated on a 3% agarose gel and stained with ethidium bromide for visualization.

Histological analysis

The cells from fresh and frozen bone were also examined by transmission electron microscopy (TEM). Fresh specimens were pre-fixed with 0.1 M cacodylate buffer containing 4% paraformaldehyde and 2.5% glutaraldehyde, and then post-fixed with 2% osmium tetraoxide in 0.1 M cacodylate buffer and embedded in Quetol 651 resin (Nissin EM Corp., Tokyo, Japan) according to the manufacturer's instructions. In addition, to evaluate the structure of bone cells in the frozen state, bones were fixed using a freeze-substitution method, as previously described (Park et al. 2009). Briefly, bones were first transferred to acetone containing 2% osmium tetroxide (OsO_4) cooled at −80°C, and then stored at −80°C for 1 week. For freeze-substitution, the temperature was elevated stepwise from −20°C for 3 days to 4°C for 3 days. The bones were then added to acetone and washed once with cacodylate buffer at room temperature and embedded in Quetol 651 resin. Cross and longitudinal sections were prepared using an Ultracut UCT ultramicrotome (Leica, Deutsch), stained with 3.5% uranyl acetate and lead citrate, and examined with a transmission electron microscope (Hitachi H-8100; Hitachi, Hitachinaka, Japan).

Mechanical testing of tendons

Bone-patellar tendon-bones (BTBs) from both knees of 24 rats were harvested and divided into three groups: (a) FT0, in which BTBs were fresh; (b) FT1, in which BTBs were frozen using an ultra-low temperature freezer and stored at −80°C for 3 weeks; and (c) FT5, in which BTBs were repeatedly frozen and thawed five times. Immediately prior to testing, all BTBs were allowed to thaw at room temperature in PBS for 3 h. For mechanical testing, we analyzed eight BTB specimens in each group as previously described (Park et al. 2009). Briefly, tendons of BTBs from each group were trimmed to 1 mm in width and their free length was measured using a micrometer caliper. The cross-sectional areas of the tendons were calculated by measuring the width and thickness. The BTB specimens were then mounted using a 27-gauge injection needle in a specially designed device containing resin (OSTRON II; GC Dental Products Corp., Aichi, Japan) to maintain 30° of flexion to the patellar tendon in the sagittal plane and to fix the axis of loading to match that of the patellar tendon. The specimens were tested to failure on a universal testing machine at a strain rate of 9 mm/min, with force detected using a load cell (Showa Measuring Instruments Inc., Tokyo, Japan) with a maximum capacity of 50 N to obtain load deformation curves. Stress–strain curves were then calculated from the load-deformation curves. The mode of failure was noted as a break at the mid-substance of the tendon, because nearly all rat patellar tendons were broken at mid-substance under our experimental conditions, regardless of the number of freeze–thaw cycles, strain rate, and temperature. Ultimate stress, Young's modulus, and strain at failure were obtained from the stress–strain curves. Ultimate stress was defined as the peak force of the stress–strain curves, while Young's modulus was calculated using the most linear portion of the failure curve.

Statistical analysis

A multiple comparison test based on Ryan's method was used to evaluate significant differences among survival rates of the three groups. The significance level was set at 0.008 in this study. To compare the mechanical properties of the tendons between the three groups, statistical assessment was performed using one-way analysis of variance (ANOVA) with Tukey's multiple test. A P value of <0.05 was considered statistically significant.

Results

Cell morphology of cells isolated from bone

After the isolation of bone cells from femora and tibiae of 10-week-old male Wistar rats, we examined

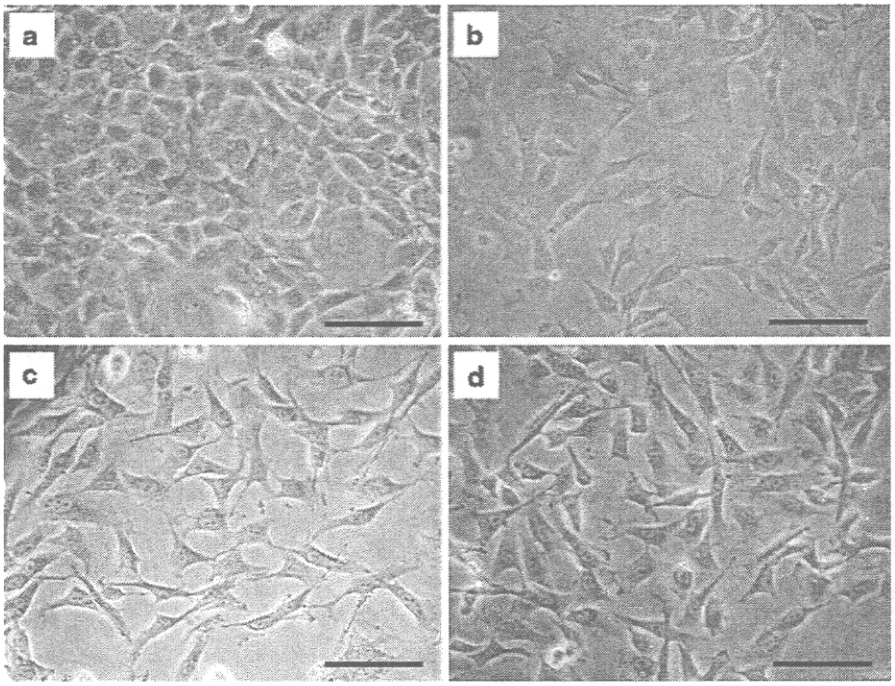

Fig. 1 Cell morphology of cells isolated from rat femoral and tibial bones. Phase-contrast microscopic images of isolated bone cells from two freeze–thaw (FT) treatment groups. **a** Osteoblastic cells in FT0, **b** osteocytic cells in FT0, **c** osteocytic cells in FT1. **d** Osteocytic cells in FT3. The scale bars indicate 100 μm

adherent cells to type I collagen-coated culture dishes by phase-contrast microscopy (Fig. 1). The cells in Fr 5, 6, and 7 that were isolated from bone samples without freeze–thaw treatment (FT0) showed two types of morphologies. Approximately half of the cells displayed an osteoblastic morphology and appeared spherical to slightly flattened, which when assembled, appeared cuboidal and displayed a cobble-stone pattern (Fig. 1a). The other type of adherent cells showed osteocytic morphology with a high cytoplasm-to-nucleus ratio, and developed extensive radial cell processes and contacted adjacent cells (Fig. 1b). In Fr 5, 6, and 7, which were obtained from cell suspensions subjected to either one or two freeze–thaw cycles (FT1 and 2, respectively), nearly all cells had a similar morphology to the osteocytic cell type in Fr 5, 6, and 7 isolated from FT0 (Fig. 1c, d).

Expression of osteoblast- and osteocyte-related marker genes

To further characterize the isolated adherent bone cells, the expression of cell-marker genes was analyzed by RT–PCR. The bone cells in Fr 5, 6, and 7 isolated from FT0 expressed several osteoblast-related marker genes, including ALP, PTHr, COL1A1, and OCN (Fig. 2). These cells also expressed the osteocyte-related gene SOST. The expression of DMP-1 was detected in Fr 5 isolated from FT0. The cells in Fr 5, 6, and 7 isolated from FT1 expressed ALP, PTHr, COL1A1, and DMP-1, but the expression of OCN and SOST was not detected. Our preliminary data showed that expression of OCN and SOST increased in a cell density-dependent manner, whereas higher expression levels of DMP-1 were observed at lower cell densities (data not shown).

TEM of bone cells

In an attempt to reveal the survival mechanisms of cells in frozen bone tissue, we next observed the cell morphology of isolated osteoblasts and osteocytes in fresh and frozen states using TEM (Fig. 3). In a fresh state, osteoblasts were flattened along bone surfaces and nuclei located at the distal end of cells could be observed (Fig. 3a). In addition, their cytoplasm contained abundant rough endoplasmic reticulum and numerous free

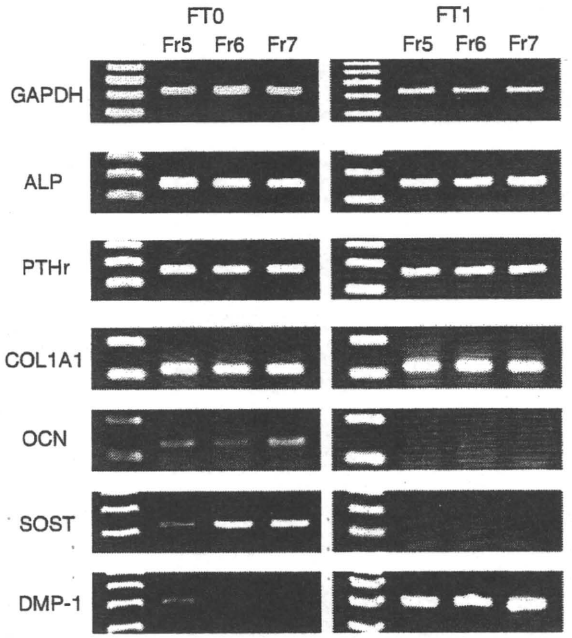

Fig. 2 Expression of osteoblast- and osteocyte-related marker genes. RT–PCR was used to analyze the expression of the indicated cell-marker genes in bone cells isolated in fraction (Fr) 5–7 from the freeze–thaw (FT) groups FT0 and FT1. GAPDH, glyceraldehydes-3-phosphate dehydrogenase; *ALP* alkaline phosphatase, *PTHr* parathyroid hormone receptor, *COL1* alpha-1 type I collagen, *OCN* osteocalcin, *SOST* sclerostin, and *DMP-1* dentin matrix protein 1

ribosomes and mitochondria were also detected. After subjecting osteoblasts to freeze-substitution, nearly all frozen cells were shrunk and contained condensed chromatin granules densely arranged around the inner rim of the nuclear membrane (Fig. 3b). In these cells, the nuclear envelope and cytoplasmic membrane appeared broken down and disrupted.

In contrast to osteoblasts, freshly isolated osteocytes appeared more rounded with relatively large nuclei (Fig. 3c). Cell organelles, such as lysosomes and rough endoplasmic reticulum were clearly observed. In the frozen state, numerous shrunken osteocytes contained condensed chromatin granules that were arranged densely at the inner rim of the nuclear membrane, similar to osteoblasts, but the distribution was more sparse and typically located in the center of the nucleus (Fig. 3d). In addition, a number of frozen cells had nuclear envelopes that were disrupted and clearly destroyed. However, several cells maintained relatively large nuclei without cytoplasmic shrinkage, and double layers of nuclear membrane without any interruption were also observed.

Effect of freeze–thaw cycle number on cell survival rate in bone and tendons

Following the isolation and culture of cells from rat femora and tibiae, it was confirmed that surviving cells were present in all fractions from each of the eight bone samples in the FT0 group (8/8) (Table 2). Upon a single freeze–thaw treatment, however, the cell survival rate in Fr 1 from FT1 (2/8) was significantly lower compared with Fr 1 from FT0 (8/8) ($P < 0.008$). An additional cycle of freeze–thawing further reduced the cell survival rate, with no viable cells observed in Fr 1 (0/8) and only limited survival in Fr 2 (2/8) from FT2 ($P < 0.008$). The cell survival rate in Fr 3 to 7 from FT2 also decreased, however, the differences were not statistically significant from Fr 3 to 7 of the FT0 group. Subjecting the isolated bone cells to a third round of freeze–thawing drastically reduced the cell survival rate, as all fractions from FT3 showed significantly decreased survival compared with FT0 ($P < 0.008$) and no detectable surviving cells in the first three fractions (Fr 1–3; 0/0).

Finally, the survival of cells harvested from tendons in the FT0 and FT1 were compared after variable incubation times after freeze–thaw treatment (Table 3). Similar to the isolated bone cells, while tendon-derived adherent cells were observed in all samples of the FT0 group, no adherent cells in the FT1 group were detected after 4-, 8-, or 18-h incubation periods (Table 3).

Mechanical properties of tendons

To compare the effects of freeze–thawing on the mechanical properties of tendons, BTB samples from the three freeze–thaw treatment groups were assayed by the tensile failure test (Table 4). Tendon failure in all BTB samples occurred at the mid-substance under our experimental conditions. The ultimate stress, Young's modulus profiles, and strain at failure showed no significant differences among the FT0, FT1, and FT5 groups.

Discussion

We examined the survival rate of cells isolated from rat bones and tendons that were subjected to freeze–

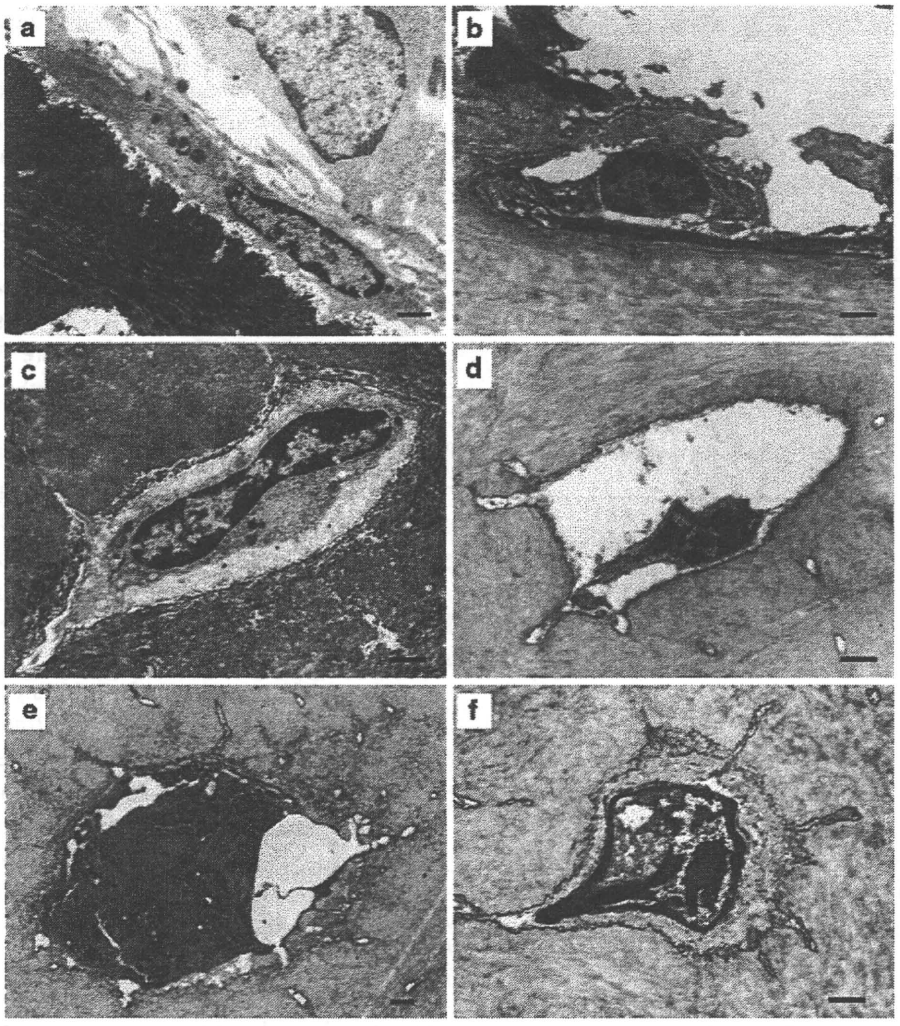

Fig. 3 Transmission electron microscopic images of bone cells in fresh and frozen states. **a** Osteoblastic cell in a fresh state. **b** Osteoblastic cell in a frozen state. **c** Osteocytic cell in a fresh state. **d–f** Osteocytic cells in a frozen state. The *scale bars* indicates 1 μm

thaw treatment. Results showed that tendon cells were completely killed by a single freeze–thaw cycle, whereas bone cells exhibited a relatively high survival rate, although the cell survival rate was significantly reduced after three freeze–thaw cycles. Nearly all cells isolated from femora and tibiae after a single freeze–thaw cycle appeared morphologically as osteocytes and expressed both osteoblast- and osteocyte-related genes. TEM images of freeze-substituted bone revealed that a number of osteocytes maintained large intact nuclei and cytoplasm, indicating that a portion of osteocytes in bone matrix were resistant to ice crystal formation. In addition, although tendon cells were completely killed after freezing, five consecutive freeze–thaw cycles did not affect the mechanical properties of tendons.

Previous studies have shown that freshly frozen human femoral head allografts contain viable cells upon thawing that are morphologically indistinguishable from those cultured from freshly harvested trabecular bone, and display similar mRNA profiles with respect to osteoblast-related gene expression (Simpson et al. 2007). In our present investigation involving femoral and tibial bones from Wistar rats, surviving cells could be cultured from freshly frozen bone. Nearly all of the isolated cells were morphologically characterized as osteocytes and were indistinguishable from fresh bone-derived osteocytic cells.

Table 2 Effect of freeze-thaw cycle number on cell survival rate in bone

	Fr 1	Fr 2	Fr 3	Fr 4	Fr 5	Fr 6	Fr 7
FT0	8/8	8/8	8/8	8/8	8/8	8/8	8/8
FT1	2/8*	8/8	8/8	8/8	8/8	8/8	8/8
FT2	0/8*	2/8*	3/8	3/8	3/8	4/8	3/8
FT3	0/8*	0/8*	0/8*	1/8*	1/8*	2/8*	2/8*

FT Freeze–thaw, *Fr* fraction

* Nominal significance level for FT0 ($P < 0.008$)

Table 3 Effect of a single freeze–thaw cycle on cell survival rate in tendons

Group	Incubation time (h)		
	4	8	18
FT0	5/5	5/5	5/5
FT1	0	0	0

FT Freeze–thaw

Although the cells isolated from frozen bone expressed both osteoblast- and osteocyte-related genes, the expression of OCN, DMP-1, and SOST was only observed in cells isolated from untreated bone samples. Expression profiles of OCN, DMP-1 and SOST may be affected by cell density rather than cell phenotype, because cell survival rates decrease with freeze–thawing treatment. Our results suggest that not only osteoblasts, but also osteocytes, survive in freeze–thawed bone.

Moreover, we also examined cell morphology in the frozen state to reveal the survival mechanisms of cells in frozen bone tissue. TEM images of bone cells subjected to a freeze-substitution method revealed that subcellular organelles in many cells were destroyed by ice crystals (Fig. 3). Surprisingly, a small percentage of osteocytes maintained relatively large nuclei with double-layered membranes and intact cell membranes and cytoplasm. Suspended and adherent cells were nearly completely killed by freeze–thawing in the absence of cryoprotectant (Shimada 1977). We speculate that the bone microenvironment, particularly the bone matrix which surrounds osteocytes provides protection from cryoinjury, such as the damage caused by ice crystal formation and salt injury. The importance of the bone matrix for protection is also supported by the fact that no cells survived in tendons after freezing, and indicates the matrix plays a role in the survival mechanism of osteocytes, which were the predominant cells isolated after the freeze–thaw treatment of bone.

Several studies have reported that surviving cells in allograft tissue are potentially immunogenic (Enneking 1957; Chalmers 1959; Langer et al. 1975). For example, Rodeo et al. (2000) reported that class-I and -II major histocompatibility complex antigens persist on cells of a meniscus prepared for transplantation even after two freeze–thaw cycles. It is therefore considered that the complete killing of cells is important for successful allogenic transplantations. Compared to a single freeze–thaw treatment, the repeated freeze–thaw of tissues, including the palate, liver, and skin, is known to produce more extensive and thorough tissue destruction and increase necrosis (Gage and Baust 1998). Here, we found that tendon cells were completely killed by a single freeze–thaw cycle, while bone cells were significantly reduced after three freeze–thaw cycles. Cryobiological research has demonstrated that all parts of the freeze–thaw cycle, particularly the cooling and warming rates, are associated with tissue destruction and cell injury (Gage and Baust 1998). For example, intracellular ice crystal formation is more likely to occur with rapid cooling rates (Gage and Baust 1998). As we have demonstrated that osteocytes survive even after three consecutive freeze–thaw cycles, further investigation is needed to reveal the conditions required for complete disappearance of allograft immunogenicity using freeze–thaw cycles.

Table 4 Mechanical properties of tendons subjected to freeze–thaw treatment

FT freeze thaw

All values are presented as the mean ± SD

Group	Number of samples	Ultimate stress (MPa)	Young's modulus (MPa)	Strain at failure (%)
FT0	8	42.6 ± 16.3	206.8 ± 99.2	22.0 ± 4.8
FT1	8	30.7 ± 17.8	185.0 ± 119.4	17.4 ± 4.1
FT5	8	46.1 ± 17.9	211.4 ± 108.3	23.8 ± 4.9

The initial strength of tendons used for transplantation is important for successful ACL reconstruction. Several studies have reported that the various procedures used for tendon allograft preparation, such as freezing and irradiation, adversely affect the mechanical properties of tendons (Clavert et al. 2001; Fideler et al. 1995; Noyes and Grood 1976). Conflicting results regarding the effects of cryopreservation on the mechanical properties of tendons have been reported, with several studies stating that mechanical properties are not affected (Nikolaou et al.1986; Noyes and Grood 1976; Woo et al. 1986), while others have indicated that biomechanical changes did occur (Clavert et al. 2001; Smith et al. 1996). Although we previously found that the mechanical properties of rat tendons subjected to a single freeze–thaw cycle were not significantly different than those of fresh tendons (Park et al. 2009). In the present study, even an additional four freeze–thaw cycles did not significantly decrease the mechanical properties of rat tendons. Our previous study showed that many spaces were present in the interfibrillar substance of tendons, and collagen fibrils were divided and squeezed by these spaces in the frozen state. However, such spaces and ice crystal formation were not observed in freeze–thawed tendons (Park et al. 2009). In addition, we did not observe significant differences in the fibril occupation ratio and cycle length of intraperiodic bands of collagen fibrils between the control and freeze–thawed tendons. Taken together, these results suggest that repeated freeze-thaw cycles may not significantly affect the mechanical properties of tendons.

A number of studies using animal models, including dogs, monkeys, and rats, have shown that mechanical of tendons failure mostly occurs at tibial insertion sites during tensile testing (Clavert et al. 2001; Noyes and Grood 1976; Shino et al. 1984; Su et al. 2008). Our preliminary experiments also revealed that nearly all BTBs failed at tibial insertion sites when the tibial tuberosity was maintained at 0° of flexion to the patellar tendon in the sagittal plane (data not shown). We previously attempted to optimize experimental conditions to evaluate the mechanical properties of tendon substances and found that failure of tendons reproducibly occurred at mid-substance with when the tibial tuberosity was held at 30° of flexion to the patellar tendon in the sagittal plane. Here, we therefore evaluated the effects of repeated freeze-thaw cycles on tendon substances under these previous experimental conditions. In clinical situations, cruciate ligament ruptures occur not only in mid-substance, but also at insertion sites. Thus, further investigation under other experimental conditions may be needed to confirm the applicability of our current findings to clinical situations.

In conclusion, we found that surviving cells in rat femoral and tibial bones subjected to freeze-thawing consisted of not only osteoblasts, but also significant numbers of osteocytes. We demonstrated that tendon cells were completely killed by a single freeze-thaw cycle, while bone cells displayed relatively high survival rates, although survival was significantly reduced after three freeze-thaw cycles. Significantly, five consecutive freeze-thaw cycles did not affect the mechanical properties of rat tendons in this experiment.

Acknowledgments This investigation was supported in part by grants-in-aid from the Ministry of Education, Sports, Culture, Science, and Technology of Japan and by grants-in-aid from the Ministry of Health, Labour, and Welfare, Japan for Research on Human Genome, Tissue Engineering, and Food Biotechnology to M. I.. This research was also supported by grants-in-aid from the Ministry of Education, Sports, Culture, Science, and Technology of Japan to K. N. and K. U., and by research grants from the Parents' Association of Kitasato University School of Medicine, the Nakatomi Foundation, and SDS Inc. to K. N.

References

Barrett DS (1991) Proprioception and function after anterior cruciate reconstruction. J Bone Joint Surg Br 73:833–837

Beynnon BD, Johnson RJ, Fleming BC, Kannus P, Kaplan M, Samani J, Renstrom P (2002) Anterior cruciate ligament replacement comparisn of bone-patellar tendon-bone grafts with two-strand hamstring grafts. A prospective, randomized study. J Bone Joint Surg Am 84A:1503–1513. doi:10.1007/s00421-008-0955-8

Chalmers J (1959) Transplantation immunity in bone homografting. J Bone Joint Surg Br 41-B:160–179

Clavert P, Kempf JF, Bonnomet F, Boutemy P, Marcelin L, Kahn JL (2001) Effects of freezing/thawing on the

biomechanical properties of human tendons. Surg Radiol Anat 23:259–262. doi:10.1007/s00276-001-0259-8

Dilley AV, Dy DY, Warlters A, Copeland S, Gillies AE, Morris RW, Gibb DB, Cook TA, Morris DL (1993) Laboratory and animal model evaluation of the Cryotech LCS 2000 in hepatic cryotherapy. Cryobiology 30:74–85. doi:10.1006/cryo.1993.1007

Enneking WF (1957) Histological investigation of bone transplants in immunologically prepared animals. J Bone Joint Surg Am 39-A:597–615

Fideler BM, Vangsness CT Jr, Lu B, Orlando C, Moore T (1995) Gamma irradiation: effects on biomechanical properties of human bone-patellar tendon-bone allografts. Am J Sports Med 23:643–646. doi:10.1177/036354659502300521

Gage AA, Baust J (1998) Mechanisms of tissue injury in cryosurgery. Cryobiology 37:171–186. doi:10.1006/cryo.1998.2115

Gill W, Fraser J, Carter DC (1968) Repeated freeze-thaw cycles in cryosurgery. Nature 219:410–413. doi:10.1038/219410a0

Gitelis S, Cole BJ (2002) The use of allografts in orthopaedic surgery. Instr Course Lect 51:507–520

Heyligers IC, Klein-Nulend J (2005) Detection of living cells in non-processed but deep-frozen bone allografts. Cell Tissue Bank 6:25–31. doi:10.1007/s10561-005-1089-4

Kleipool AE, Zijl JA, Willems WJ (1998) Arthroscopic anterior cruciate ligament reconstruction with bone-patellar tendon-bone allograft or autograft. A prospective study with an average follow up of 4 years. Knee Surg Sports Traumatol Arthrosc 6:224–230. doi:10.1007/s001670050104

Langer F, Czitrom A, Pritzker KP, Gross AE (1975) The immunogenicity of fresh and frozen allogeneic bone. J Bone Joint Surg Am 57:216–220

Mikuni-Takagaki Y, Kakai Y, Satoyoshi M, Kawano E, Suzuki Y, Kawase T, Saito S (1995) Matrix mineralization and the differentiation of osteocyte-like cells in culture. J Bone Miner Res 10:231–242. doi:10.1002/jbmr.5650100209

Naruse K, Mikuni-Takagaki Y, Azuma Y, Ito M, Oota T, Kameyama K, Itoman M (2000) Anabolic response of mouse bone-marrow-derived stromal cell clone ST2 cells to low-intensity pulsed ultrasound. Biochem Biophys Res Commun 268:216–220. doi:10.1006/bbrc.2000.2094

Naruse K, Urabe K, Mukaida T, Ueno T, Migishima F, Oikawa A, Mikuni-Takagaki Y, Itoman M (2004) Spontaneous differentiation of mesenchymal stem cells obtained from fetal rat circulation. Bone 35:850–858. doi:10.1016/j.bone.2004.05.006

Nikolaou PK, Seaber AV, Glisson RR, Ribbeck BM, Bassett FH III (1986) Anterior cruciate ligament allograft transplantation. Long-term function, histology, revascularization, and operative technique. Am J Sports Med 14:348–360. doi:10.1177/036354658601400502

Noyes FR, Grood ES (1976) The strength of the anterior cruciate ligament in humans and Rhesus monkeys. J Bone Joint Surg Am 58:1074–1082

Park HJ, Urabe K, Naruse K, Onuma K, Nemoto N, Itoman M (2009) The effect of cryopreservation or heating on the mechanical properties and histomorphology of rat bone-patellar tendon-bone. Cell Tissue Bank 10:11–18. doi:10.1007/s10561-008-9109-9

Rodeo SA, Seneviratne A, Suzuki K, Felker K, Wickiewicz TL, Warren RF (2000) Histological analysis of human meniscal allografts. A preliminary report. J Bone Joint Surg Am 82-A:1071–1082

Scutt N, Rolf CG, Scutt A (2008) Tissue specific characteristics of cells isolated from human and rat tendons and ligaments. J Orthop Surg Res 3:32. doi:10.1186/1749-799X-3-32

Shimada K (1977) Effect of cryoprotective addictives on intracellular ice formation and survival in very rapidly cooled Hela cells. Contrib Inst Low Temp Sci 19:49–70

Shino K, Kawasaki T, Hirose H, Gotoh I, Inoue M, Ono K (1984) Replacement of the anterior cruciate ligament by an allogeneic tendon graft. An experimental study in the dog. J Bone Joint Surg Br 66:672–681

Simpson D, Kakarala G, Hampson K, Steele N, Ashton B (2007) Viable cells survive in fresh frozen human bone allografts. Acta Orthop 78:26–30. doi:10.1080/17453670610013385

Smith CW, Young IS, Kearney JN (1996) Mechanical properties of tendons: changes with sterilization and preservation. J Biomech Eng 118:56–61

Su WR, Chen HH, Luo ZP (2008) Effect of cyclic stretching on the tensile properties of patellar tendon and medial collateral ligament in rat. Clin Biomech (Bristol., Avon.) 23:911–917

Uchida K, Urabe K, Naruse K, Ujihira M, Mabuchi K, Itoman M (2007) Comparison of the cytokine-induced migratory response between primary and subcultured populations of rat mesenchymal bone marrow cells. J Orthop Sci 12:484–492. doi:10.1007/s00776-007-1159-5

Weyts FA, Bos PK, Dinjens WN, van Doorn WJ, van Biezen FC, Weinans H, Verhaar JA (2003) Living cells in 1 of 2 frozen femoral heads. Acta Orthop Scand 74:661–664. doi:10.1080/00016470310018162

Woo SL, Orlando CA, Camp JF, Akeson WH (1986) Effects of postmortem storage by freezing on ligament tensile behavior. J Biomech 19:399–404